Characterization and Modeling of Microstructure Development in Nickel-base Superalloy Welds[†]

1. S. S. Babu — Oak Ridge National Laboratory, Oak Ridge, TN 37831.
2. S. A. David — Oak Ridge National Laboratory, Oak Ridge, TN 37831.
3. J. M. Vitek — Oak Ridge National Laboratory, Oak Ridge, TN 37831.
4. M. K. Miller — Oak Ridge National Laboratory, Oak Ridge, TN 37831.

This manuscript was authored by a contractor of the U.S. Government under contract no. DE-AC05-96OR22464. Accordingly, the U.S. Government retains a nonexclusive, royalty-free license to publish or reproduce the published form of the contribution, or allow others to do so, for U.S. Government purposes.

[†] The research was sponsored by the Division of Materials Sciences, U.S. Department of Energy, under contract DE-AC05-96OR22464 with Lockheed Martin Energy Research Corporation.

Introduction

Welding is important for economical reuse and reclamation of used and failed nickel-base superalloy blades, respectively [1]. Solidification and solid state decomposition of γ (Face Centered Cubic, FCC) phase into γ' ($L1_2$-ordered) phase control the properties of these welds. In previous publications, the microstructure development in electron beam welds of PWA-1480 alloy [2] and laser beam welds of CMSX-4 alloy [3] were presented. These results showed that the weld cracking in these alloys were associated with low melting point eutectic at the dendrite boundaries [1, 2]. The eutectic-γ' precipitation was reduced at rapid weld cooling rates and the partitioning between γ-γ' phase was found to be far from equilibrium conditions [3, 4]. This observation was related to diffusional growth of γ' precipitate into γ phase. Subsequent to the above work, the precipitation characteristics of γ' phase from γ phase were evaluated during continuous cooling conditions [5]. The results show that the number density of γ' precipitates increased with an increase in cooling rate. However, the details of this decomposition and also the fine-scale elemental partitioning characteristics between γ-γ' were not investigated. In this paper, the precipitation characteristics of γ' from γ during continuous cooling conditions were investigated with transmission electron microscopy, and atom probe field ion microscopy. In addition, thermodynamic and kinetic models were used to describe microstructure development in Ni-base superalloy welds.

Experiment

A directionally solidified Ni-base superalloy CM247DS (Ni - 12.1 at. % Al - 9.12% Cr - 9.05% Co - 1.0% Ti - 0.06% Nb - 0.37% Mo - 1.05% Ta - 3.06% W - 0.4% C) was used in this investigation. The alloy was subjected to continuous cooling heat treatments in a Gleeble® thermomechanical simulator. The relative radius change of the sample was monitored using dilatometry. The heat treatments include 5-min hold at a solutionizing temperature of 1300°C and continuous cooling at rates of 0.17 to 75°Cs^{-1}. In addition, the samples were water quenched from 1300°C.

An atom probe field-ion microscope [6] was used to characterize the water-quenched sample. For APFIM, small needles were machined from the sample. These needles were electropolished using standard techniques. The samples were imaged at a temperature range of 50 to 60 K and analyzed with a residual neon gas pressure of 3×10^{-7} Pa and a pulse fraction of 20% in the atom probe.

To evaluate the decomposition characteristics of CM247DS alloy, thermodynamic calculations were performed with ThermoCalc® software [7]. The calculations describe multi-component and multi-phase thermodynamic equilibrium. The calculations used an 11-element Ni-Fe database [8]. The alloying elements considered in the calculations were Ni, Al, Nb, Ti, Cr, Co, Mo, and C. The calculations ignored the effects of Ta and W due to the limitation of the database.

Diffusion controlled kinetics of γ phase solidification, as well as, γ' precipitate growth into γ phase during continuous cooling was simulated with DicTra® software [9]. In these simulations, thermodynamic local equilibrium at the phase boundaries was calculated with the Ni-Fe database [8]. Moreover, the diffusion in γ' phase was ignored and as a result the kinetics are controlled only by the diffusion in the γ phase.

Results and Discussion

Microstructure Development during Continuous Cooling: Transmission electron micrographs of the samples subjected to continuous cooling are compared in Fig. 1. The micrographs show that with an increase in cooling rate, the number density of γ' precipitates increased and the size of γ' precipitates decreased. This result is consistent with that of MacKay and Ebert [10], in which the γ' precipitate size decreased on changing the cooling conditions from forced air cooling to oil quenching in Ni - Al - Ta - Mo alloys.

In the present work, in addition to an increase in the number density of γ' precipitates, their shape changed with increasing cooling rate. The micrographs in Fig. 1 show cuboidal γ' precipitates at slow cooling rates and their shape progressively becomes irregular and approaches a spherical morphology in the water-quenched sample. Analysis of the microstructure cooled at $0.17°Cs^{-1}$ showed that the size of the γ' precipitates is larger than that of base metal. In this condition, the γ' precipitates exhibited morphology that is consistent with the coarsening stage. High-magnification

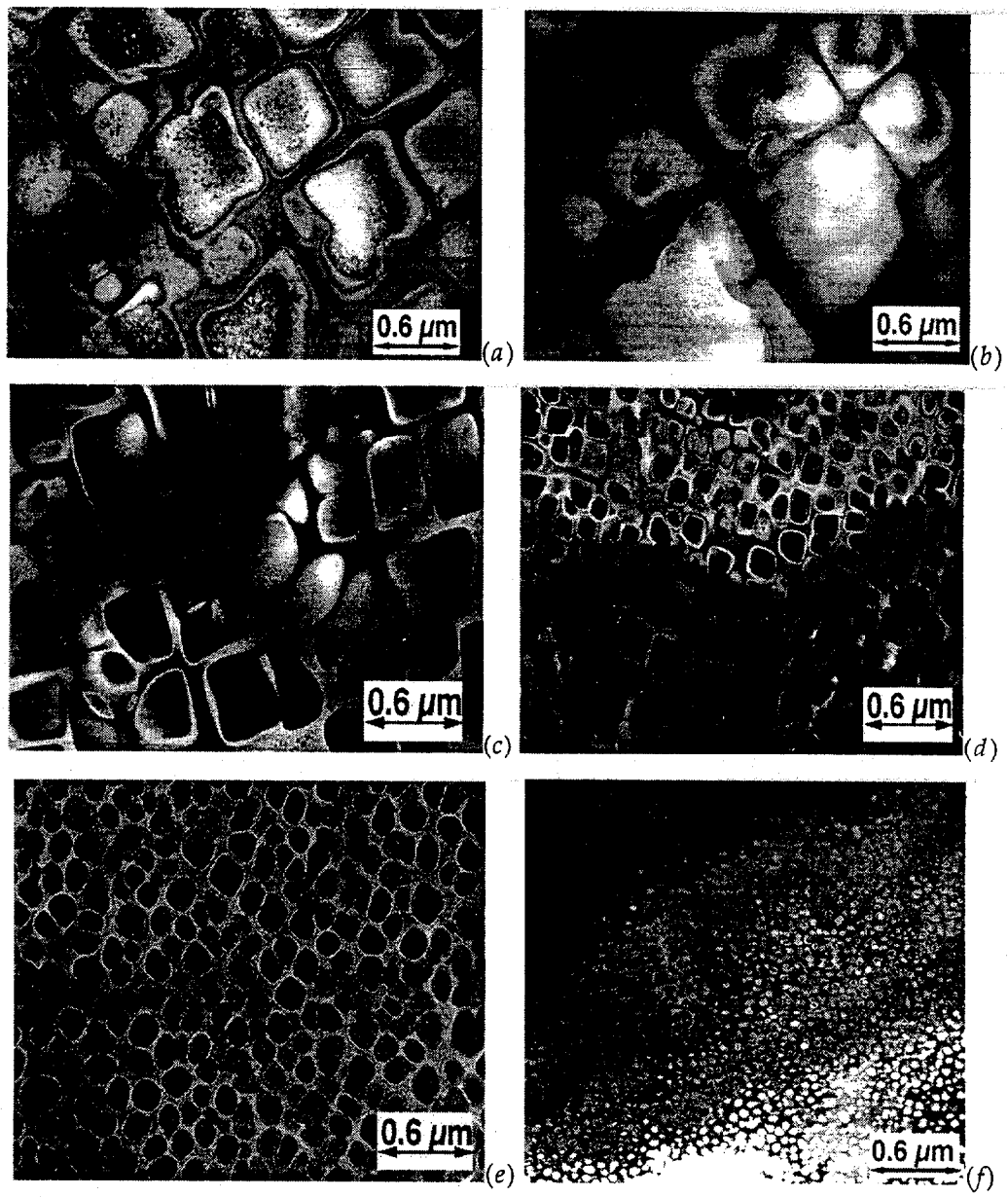

Fig. 1 Transmission electron micrographs of CM247DS samples subjected to different heat treatments imaged in [001] zone axis (*a*) as received, (*b*) $0.17°Cs^{-1}$, (*c*) $1°Cs^{-1}$, (*d*) $10°Cs^{-1}$, (*e*) $75°Cs^{-1}$, and (*f*) water quenched.

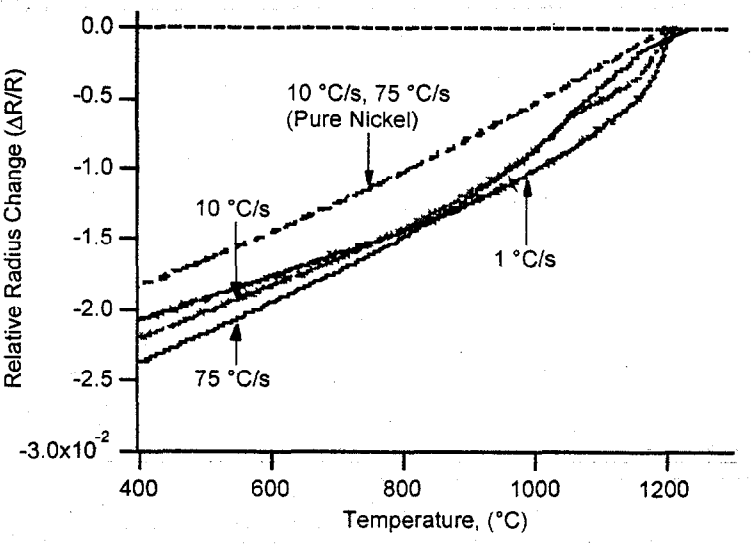

Fig. 2 Comparison of measured relative radius change for CM247DS samples cooled at different rates compared with that of pure nickel sample [4].

micrographs of samples cooled at $1°Cs^{-1}$, revealed small amount of fine secondary γ' precipitates.

In addition to the above microstructural changes, the dilatation characteristics were different as shown in Fig. 2 [4]. In general, the dilatometry measurements are sensitive to volume change and the coefficient of thermal expansion changes due to phase transformations. The observed change in Fig. 2 is speculated to be due to the γ' formation [4, 11] at different undercooling.

An interesting observation in this work is that even under rapid cooling conditions imposed by water quenching, the precipitation of γ' precipitates could not be avoided. This result is consistent with the work of Wendt and Haasen [12] who observed the completion of γ decomposition to γ' precipitate in a Ni – 14 at. % Al binary alloy during water quenching. With APFIM concentration profiles, Wendt and Haasen concluded that in a Ni –14 at. % Al binary alloy, the decomposition occurs by a classical nucleation and growth mechanism. The observation of increased γ' precipitate number density with increased cooling rate (see Fig. 1) suggests that the decomposition of γ phase occurs by nucleation and growth mechanism in the current alloy. However, as pointed out by Wendt and Haasen, the decomposition mechanism can only be understood by measuring the composition of the γ and γ' phases. Also, it will be interesting to analyze the partitioning characteristics of heavy elements such as tungsten during such phase transformations.

Atom Probe Field Ion Microscopy of Water-Quenched Samples: The concentration profiles of Cr, Co Al and W across γ and γ' phases from the water-quenched sample are shown in Fig. 3. The concentration profiles revealed the following characteristics. There were no large concentration gradients of either Al or Cr within the γ' phase. This result is in agreement with the work of Wendt and Haasen [12] in which they observed γ' phase with an equilibrium aluminum concentration. However, in the present work, anomalous Co-enriched regions were observed within the γ' phase. Also, the concentration of W in γ phase should be higher than that of γ' phase; however, the measured concentration profiles [see Fig. 3(*b*)] show a complicated behavior. Tungsten was found in higher concentration levels in both phases. This is attributed to rapid weld cooling conditions, which does not allow for achieving equilibrium. However, the mechanism of extensive Cr, Al and Co-partitioning without the associated W-partitioning remains to be understood. The APFIM results also showed concentration gradients within the γ phase. As pointed out in the earlier work [3], the above concentration gradients will affect the lattice misfit between γ and γ' phases.

The above results support the nucleation and growth mechanism proposed by Wendt and Haasen [12] even in multicomponent nickel-base superalloys. However, it is intriguing that this decomposition occurs with diffusion of Cr, Co and Al even at rapid cooling conditions imposed by water quenching. Although, APFIM analysis provided crucial information of the γ' and γ phase, still three-dimensional distribution of these elements around a γ' precipitate is needed to understand the phase transformation mechanisms. Further work is underway to investigate these partitioning characteristics with the use of atom probe tomography [13, 14].

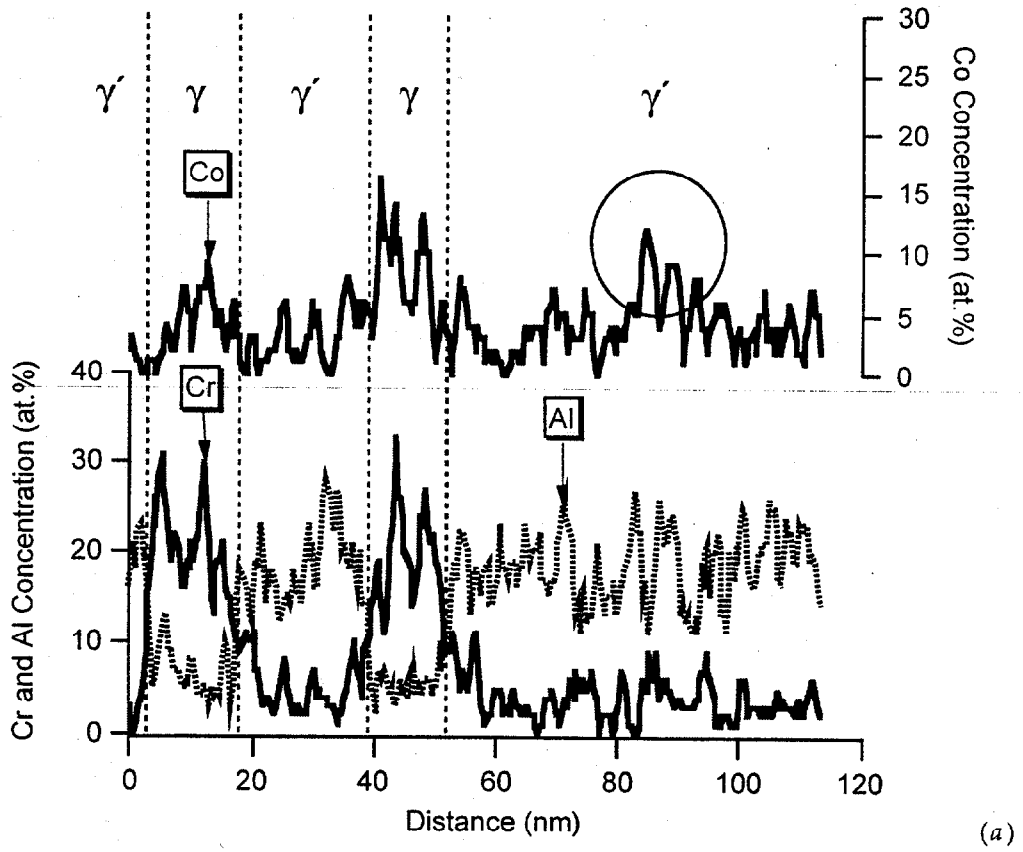

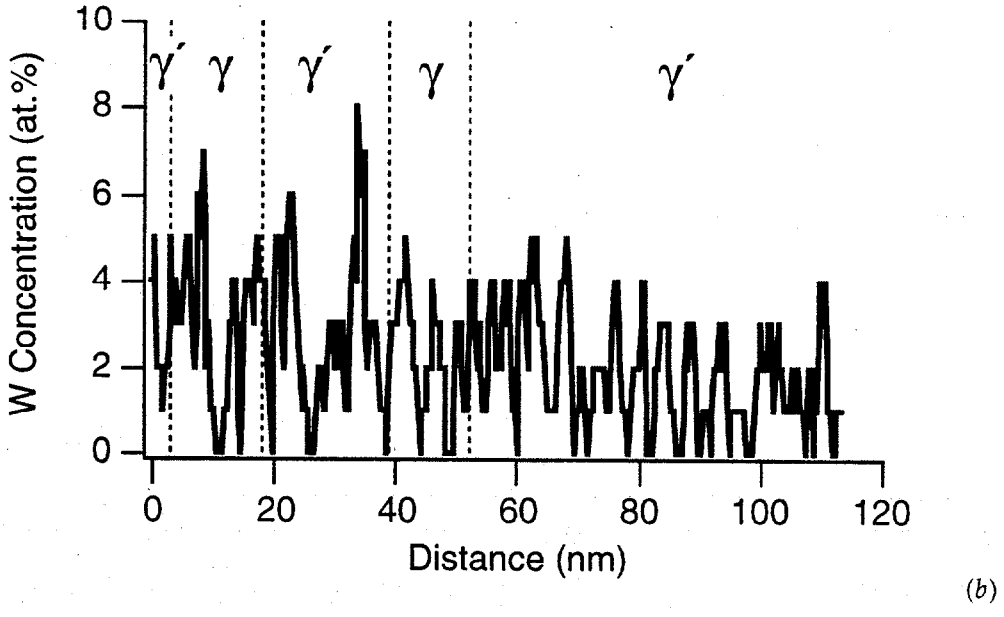

Fig. 3 APFIM concentration depth profiles of Cr, Co and Al across γ and γ´ phases from the water quenched sample. The concentration profiles within the γ´ region (circled) shows Co-enriched region and (*b*) shows concentration profile for tungsten.

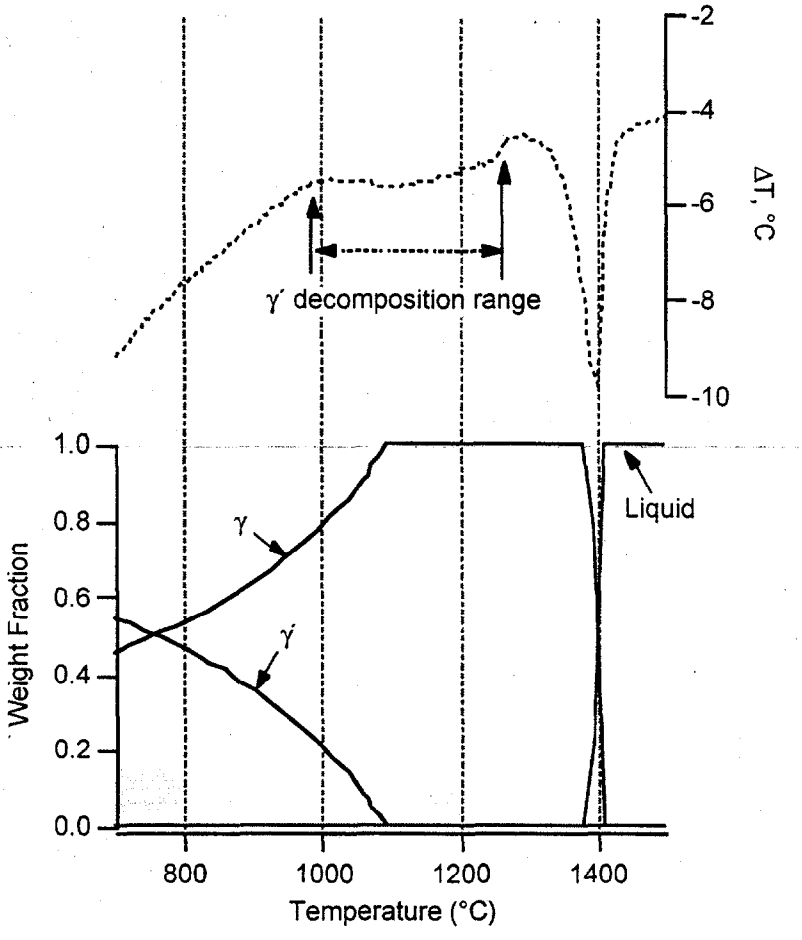

Fig. 4 Comparison of predicted equilibrium fraction of various phases as a function of temperature with DTA data obtained while heating at a rate of 0.17°Cs^{-1}. The calculations also indicated formation of small amount of $M_{23}C_6$ and TiC; however, they are not shown in the plot.

Thermodynamic and Kinetic Description of Phase Evolution: To evaluate the above mentioned microstructure development, thermodynamic and kinetic calculations were performed with ThermoCalc [7] and DicTra software [9], respectively. The first set of calculations considered the equilibrium fraction of various phases as a function of temperature for the CM247DS alloy. The phases considered in the equilibrium calculations were Ni_3Nb, TiC based carbonitride, γ (FCC), γ′($L1_2$-ordered), σ, δ′, M_6C, laves, $M_{23}C_6$, M_7C_3, and liquid. The predicted phase fraction was compared with differential thermal analysis (DTA) data in Fig. 4. The predictions indicate that the predominant microstructure in this alloy, at low temperature, is a mixture of γ and γ′ phases. However, as the temperature increases, the γ′ fraction decreases and at 1093°C, the alloy is expected to be mostly γ phase. However, the DTA data shows that the γ′ solvus temperature range extends from 1000°C to 1279°C. This difference is attributed to the kinetic constraints, including the effect of Ta and W, which was ignored in the calculations.

The next set of calculations considered the solidification of CM247DS alloy. Such calculations would allow the estimation of the freezing range of these alloys. This, in-turn, could be used to estimate the hot cracking tendency of these alloys. As a first step, the calculations considered the solidification conditions assuming Scheil additivity law. The solid fractions were determined for an alloy of Ni - 9.12 at. % Cr - 9.05% Co - 12.1% Al - 1.0%Ti as a function of temperature (see Fig. 5). In the above calculation, the diffusion in solid is ignored and the mixing in liquid is considered complete.

In the next step, the solidification simulation considered diffusion-controlled growth of γ phase into liquid as a function of cooling rate. In these calculations, two conditions were considered one with half dendrite arm spacing (HDAS) of 1μm and another one with 10μm. The geometry of the simulation is shown in Fig. 5. The

liquid composition was taken as Ni - 9.12 at. % Cr - 9.05% Co - 12.1% Al - 1.0%Ti. The simulations considered cooling from 1427°C at a rate of 1 and 100°Cs^{-1}. The calculations describe diffusion in both liquid and γ phases. The above predictions are compared in Fig. 5. The results show that the freezing range calculated assuming Scheil additivity law is larger than calculated by equilibrium assumption and diffusion controlled growth calculations. In specific, allowing for diffusion and cooling at 1°Cs^{-1} or 100°Cs^{-1}, the freezing range increased marginally from the equilibrium estimation with a dendrite arm spacing of 2μm. With a large dendrite arm spacing of 20μm, the freezing range increased for both cooling rates, but still the freezing range was less than that predicted by Scheil additivity law. This shows the diffusion is very rapid in these alloys and the freezing range may not be as large as predicted by Scheil additivity law. However, note that these calculations did not consider the effect of Ta and W.

Finally, the decomposition of γ phase through diffusion controlled growth of γ′ phase was simulated. The geometry of the sample is shown in Fig. 6. An interparticle spacing of 20 nm was assumed. This simulation was performed to evaluate the APFIM composition profiles obtained from water-quenched sample. Simulation was performed for an alloy composition of Ni - 9.12 at. % Cr - 9.05% Co - 12.1% Al - 1.0%Ti while it cools from 1090°C to 888°C at a rate of 500°Cs^{-1}. Further growth of γ′ phase into γ phase below

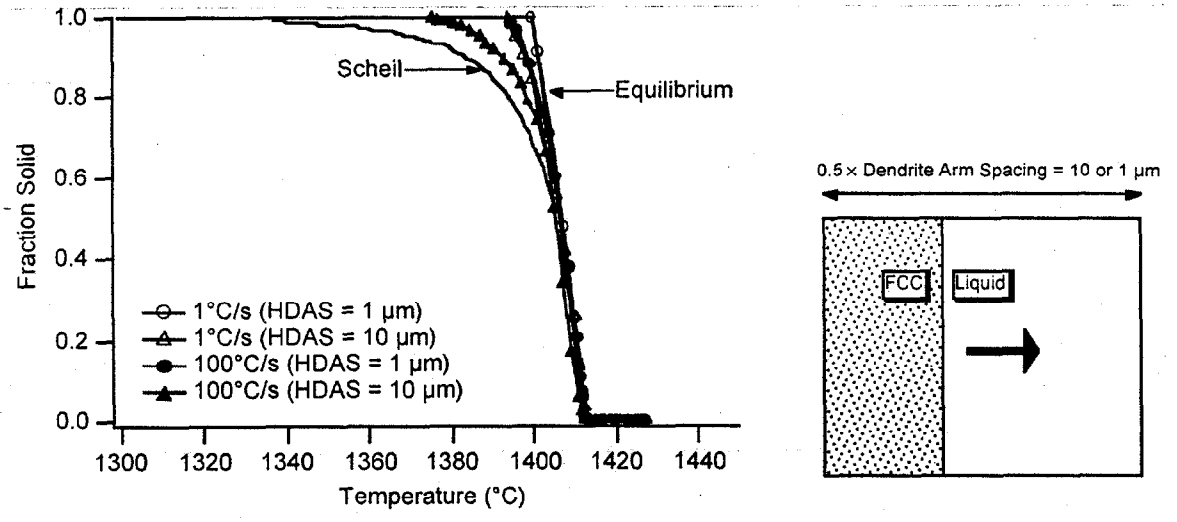

Fig. 5 Comparison of predicted solid fraction variation with temperature using equilibrium calculations, scheil additivity rule, diffusion controlled growth at 1°Cs^{-1} and 100°Cs^{-1}. The right side of the diagram shows the geometry used in the simulation.

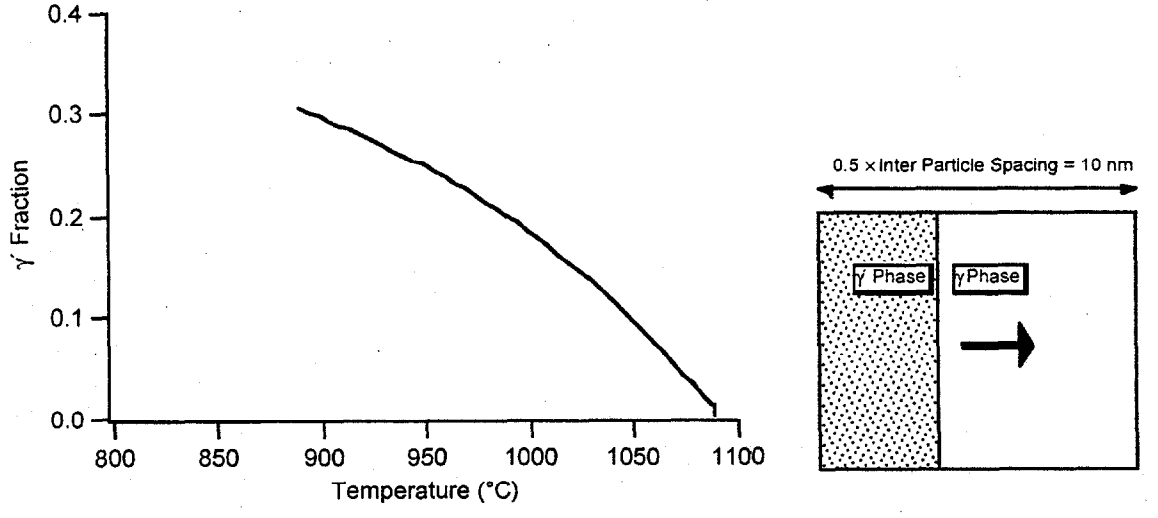

Fig. 6 Predicted variation of γ′ volume fraction with time as the alloy cools from 1090°C at a linear rate of 500°Cs^{-1}. The right side of the diagram shows the geometry used in the simulation.

888°C was ignored due to very low interface velocities in the simulation and numerical instabilities. The calculated volume fraction of γ′ with temperature for this condition is shown in Fig. 6. The results show rapid growth of γ′ into γ phase below 1090°C. The composition profiles at the end of simulation at 888°C are shown in Fig. 7. The predicted concentration profiles qualitatively agree with the observed concentration gradients in γ phase (see Fig. 3). However, the magnitudes of gradients predicted by simulations were smaller than the measured ones. For example, the predicted Cr concentrations range from 12 to 10 at. % in the γ phase. In the case of measured concentrations, they can vary as high as 30 at. % and reduces to 12 at. %. Moreover, the simulations cannot reproduce the anomalous Co-enrichment within γ phase.

It is important to note that the simulations assumed no diffusion within γ′ phase and this assumption leads to build up of small Cr concentration profiles within γ′ phase. However, the experimental concentration profiles do not exhibit such profiles. In addition, the calculations do not consider the nucleation of the γ′ and therefore, the effect of subsequent independent nucleation of γ′ on the original growth of γ′ phase needs to be evaluated in future work.

Summary and Conclusions

The γ-γ′ microstructure evolution in a CM247DS alloy during continuous cooling was investigated with TEM and APFIM. TEM revealed that the number density of γ′ precipitates increased and the size of γ′ precipitates decreased with an increase in cooling rate. With an increase in cooling rate, the shape of the γ′ precipitate became non-cuboidal and approached spherical shape. The decomposition of γ′ was complete even in water-quenching condition. APFIM of water-quenched samples showed concentration gradients within the γ phase. An anomalous Co-enriched region was detected within the γ′ region.

Thermodynamic and kinetic models were applied

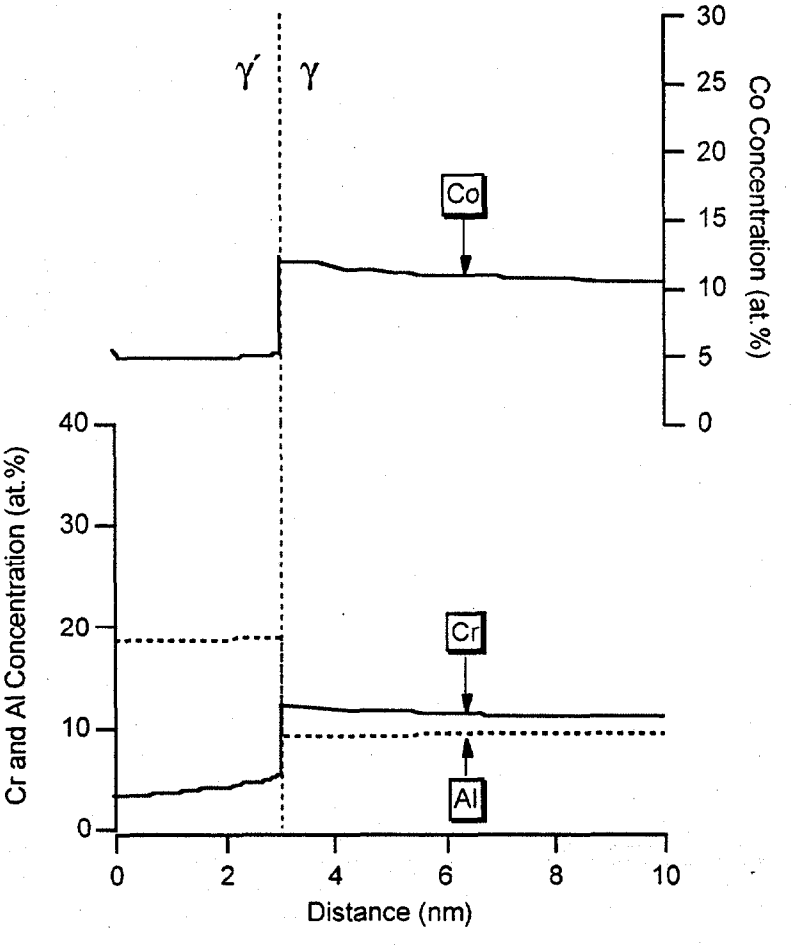

Fig. 7 Predicted concentration profiles of Cr, Co and Al at 888°C after cooling from 1090°C at a rate of 500 °C.

to describe the weld microstructure development in Ni-base superalloy welds. The calculations estimated the freezing range, as well as, the solid state decomposition of γ phase into γ' phase. Diffusion controlled growth calculations showed the freezing range in these alloys may not be large as predicted by the Scheil additivity law due to extensive diffusion in liquid and solid. In addition, the diffusion-controlled growth of γ' phase into γ phase at a rate of $500°Cs^{-1}$ was simulated and the simulation qualitatively supported the measured concentration gradients within γ phase, but the predicted magnitudes were smaller than that of measured ones.

Acknowledgments

The research was sponsored by the Division of Materials Sciences, U.S. Department of Energy, under contract DE-AC05-96OR22464 with Lockheed Martin Energy Research Corporation. The authors acknowledge the technical assistance provided by J. W. Jones, R. W. Reed and K. F. Russell. This research was conducted utilizing the Shared Research Equipment (SHaRe) User Program facilities at Oak Ridge National Laboratory.

References

1 . S. A. David, J. M. Vitek, S. S. Babu, L. A. Boatner, and R. W. Reed, *Sci. Tech. Weld. Joining*, **2**, 79-88 (1997).

2. S. S. Babu, S. A. David, and J. M. Vitek, *Appl. Surf. Sci.*, **94/95**, 280-287 (1995).

3. S. S. Babu, S. A. David, J. M. Vitek, and M. K. Miller, *J. de Physique IV*, 6, 253-258 (1996).

4. S. S. Babu, S. A. David, J. M. Vitek, and M. K. Miller, Proceedings, Trends in Welding Research, ed. Vitek et al., ASM International, Metals Park, OH, 1999, 239-244.

5. S. S. Babu, S. A. David, J. M. Vitek, and M. K. Miller, *Microscopy and Microanalysis*, **4**, 94-95, (1998).

6 . M. K. Miller, *J. de Physique*, **47**, 493-498, (1986).

7. B. Sundman, B. Jansson, and J. O. Andersson, *Calphad*, **9**, 153-190, (1985).

8. N. Saunders, "Ni-data information", Thermotech ltd., Surrey Technology Center, Guidford, Surrey, GU2 5YG, UK, 1998.

9. J. Agren, *ISIJ International*, **32**, 291-296, (1992)

10. R. A. MacKay and L. J. Ebert, Proceedings, Fifth international conference on Superalloys, ed. M. Gell et al., AIME, New York, NY, 1984, 135-144.

11. R. W. Cahn, P. A. Siemers, J. E. Geiger, and P. Bardhan, *Acta Metall.*, **35**, 2737-2751, (1987)

12. H. Wendt and P. Haasen, *Acta Metall.*, **31**,1649-1659, (1983).

13. M. K. Miller, *J. of Micros.*, **186**, 1-16, 1997.

14 . S. S. Babu, S. A. David, J. M. Vitek, and M. K. Miller, to be presented at the TMS symposium on "Advanced Technologies for Superalloys affordability," Nashville, 2000.